Derating of Induction Motors Due to Power Quality Issues Considering the Motor Efficiency Class

Pablo D. Donolo , *Member, IEEE*, Carlos M. Pezzani , *Member, IEEE*,
Guillermo R. Bossio , *Senior Member, IEEE*, Cristian H. De Angelo , *Senior Member, IEEE*,
and Marcos A. Donolo , *Senior Member, IEEE*

Abstract—**Heating and losses of induction motor (IM) grow with the supply voltage unbalance and harmonic distortion. To avoid thermal overload, the IEEE 141-1993, the IEEE 3004.8, NEMA MG1-2014, and the IEC 60034-26 standards establish derating factors for IMs operating under those conditions. In this article, we show that while the derating factors proposed by these standards adequately protect standard-efficiency IMs, they are only marginally adequate to protect modern higher-efficiency IMs. To this end, we compare the derating factors provided by the standards with the derating factors required to maintain the losses at rated values in a standard-efficiency IM, in a premium-efficiency IM, and in a super-premium-efficiency IM. To extrapolate the results from these IM, we compared the nameplate data of 548 IMs of different efficiency classes and found that higher efficiency classes correlate to higher IM starting currents and lower impedances to the negative sequence and harmonic voltages. These lower impedances in turn may lead to higher losses for unbalanced and harmonic voltages conditions.**

Index Terms—**Energy efficiency, induction motors (IMs), power quality.**

I. INTRODUCTION

ELECTRIC motors, and in particular induction motors (IMs), represent the most important load in the electric power system. Its participation in the demand for electric energy is close to half of the energy consumed globally [1], [2]. For this reason, even today, there are proposals to increase the electric motors efficiency to yield large energy savings [3].

To promote the development of more efficient IMs, the IEC 60034-30 standard from 2008 specified three efficiency classes. Compliance with these classes guarantees a minimum efficiency level for every type of IM and nominal power. These classes are: standard efficiency or IE1, high efficiency or IE2, and

premium efficiency or IE3. A later revision of this standard includes two new efficiency classes, the super-premium or IE4 and ultra-premium or IE5 [4].

Even where no commercial restrictions apply, energy prices justify the installation of IMs in higher efficiency classes because energy savings quickly repays the higher initial investment [5]. However, the US and the EU imposed restrictions to the commercialization of IMs of efficiency classes below premium (IE3) [1], [2], [4].

As a rule of thumb for full load, IE2 class IMs are 15% more efficient than IE1 IMs and IE3 IMs are 30% more efficient than IE1 IMs, similarly IE4 IMs are 45% more efficient than IE1 IMs [4]. However, losses of higher efficiency class IMs under distorted and unbalanced voltages are not fully documented. Initial studies are not conclusive: Ferreira *et al.* [6] concludes that lower IM losses lead to lower IM temperature and then to longer IM life even considering voltage unbalance and harmonic distortion operation. On the other hand there are studies suggesting that higher-efficiency IMs are more affected by voltage supply problems [7]–[9]. Van Wyk *et al.* [10] concluded that for the same level of voltage unbalance, IMs in the IE2 efficiency class generate higher negative-sequence currents than IE1 efficiency IMs. The negative-sequence currents cause a number of problems including: additional losses, torque, speed, and power oscillations, and reduction of the average electromagnetic torque. Additionally, torque oscillations may lead to a large increase in IM vibrations [11], [12].

The magnitude of these effects depends on the IMs constructive characteristics [6], [7], [13].

To avoid thermal overload, the IEEE 141-1993 and NEMA MG1-2003 establishes derating factors for IMs under unbalanced voltage conditions and for IMs operating under distorted voltage conditions. For voltage unbalanced between 1% and 5%, this standard requires derating factors between 1 and 0.75. These derating factors apply to squirrel cage and wound rotor IMs [14], [15].

IEC 60034-26 standard requires similar derating factors but with application limited to general purpose IMs with squirrel cage rotors under unbalanced voltage condition in which the average phase voltage magnitude remains at the nominal value [16].

De Abreu and Emanuel [17] claim that the derating factors proposed by standards are too conservative and that the use of such factors results in total losses below the rated IM losses. On

the other hand, Reineri *et al.* in [18] tested a wound rotor IM and concluded that the derating factors proposed by the standard were not enough to protect the IM because losses grew faster than assumed in the standard.

The effect of harmonic distortion on new higher efficiency IMs is currently under study [19], [20]. For example, Kanchan *et al.* [21] showed that feeding a 15 kW IE2 IM with a variable frequency drive reduces its efficiency mainly due to increased losses in the IMs core and parasitic currents in the rotor. The IEEE 3004.8 and NEMA MG1-2003 standards provide derating factors for IMs operating under harmonic voltage distortion conditions. For conditions where the harmonic voltage factor (HVF) is below 0.03, no derating factor is required. On the other hand, when HVF reaches a 0.115 value, a 0.7 derating factor is required [15], [22].

In a previous version of this article [23], we show that while the derating factors proposed by the standards adequately protect standard-efficiency IMs, they are only marginally adequate to protect modern higher-efficiency IMs. To this end:

1) we first show that higher efficiency class IMs are associated with higher starting currents and lower impedances to negative sequence and harmonic voltages;
2) we run lab tests on three IMs of different energy efficiency class to obtain accurate model parameters;
3) we used the models to obtain the derating factors for which IM losses remained at design values for different levels of unbalance and harmonic distortion;
4) we compare the derating factors provided by the standard with the derating factors we obtained.

In this article, we extended the analysis of the model and provided further details into the model's validation. We also included newly found bibliographical references.

II. STARTING CURRENTS FOR DIFFERENT EFFICIENCY CLASS IMS

A. Definitions

In this article, we compute the voltage unbalance using

$$\text{VUF} = \frac{|\boldsymbol{v_2}|}{|\boldsymbol{v_1}|}.100 \qquad (1)$$

where $\boldsymbol{v_1}$ and $\boldsymbol{v_2}$ are the positive and negative sequence components of the voltage. This definition is consistent with IEEE 141-1993 [14].

To compute the harmonic distortion, we use the HVF defined by

$$\text{HVF} = \sqrt{\sum_{h=5}^{h=\infty} \frac{V_{h_{pu}}^2}{h}}, \quad h = 5, 7, 11, 13 \qquad (2)$$

where V_{hpu} is the magnitude of the harmonic voltage component of order *h,* in per unit (p.u.) of the fundamental voltage magnitude. This definition is consistent with IEEE 3004.8 [22].

B. Analysis of Starting Currents

Using the starting current in p.u. to estimate the negative sequence impedance of IMs [24], we can predict the behavior
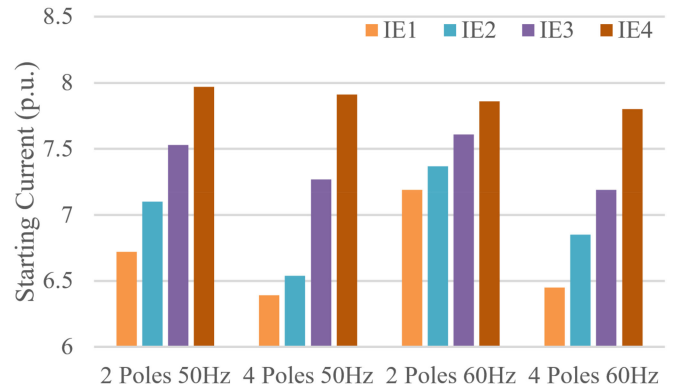

Fig. 1. Average starting current in p.u. of the rated current for IMs in different international efficiency classes at rated voltage and frequency.

TABLE I
NAMEPLATE DATA OF THE IMS

International Efficiency	IE1	IE3	IE4
Power (kW)	5.5	5.5	5.5
Voltage (V)	380	380	380
Frequency (Hz)	50	50	50
Poles	4	4	4
Frame	132	132	132
Service Factor	1	1	1
Efficiency (%)	85.5	90.7	91.9
Rated Current (A)	11.7	10.8	11.1
Rated Speed (R.P.M)	1450	1465	1470
Power Factor	0.84	0.85	0.82
Starting Current (p.u.)	7.2	8.5	8.8

of IMs losses under voltage unbalance. High starting currents imply low negative sequence impedances, leading to greater losses under unbalanced voltage conditions.

Ferreira [25] compared the starting currents of four 7.5 kW IMs, one in each of the four efficiency classes and noted that the higher the efficiency class the higher the starting current. To quantify these trend, we calculated the average starting current in p.u. for 548 IMs in different efficiency classes: 244 60 Hz IMs (75 IE1, 79 IE2, 70 IE3, 20 IE4) from 0.12 to 550 kW, and 304 50 Hz IMs (79 IE1, 90 IE2, 81 IE3, 54 IE4) form 0.12 to 500 kW (http://ecatalog.weg.net/tec_cat/tech_motor_sel_web.asp) [26]. As shown in Fig. 1, the higher the efficiency class, the higher the starting current.

These higher starting currents imply lower negative sequence impedances and higher losses under unbalanced voltage conditions [24].

As an example of this relation between the starting current and the negative sequence impedance, we tested three IMs in a laboratory setup. The IMs nameplates data are presented in Table I. The IMs are in the IE1, IE3, and IE4 efficiency class with p.u. starting currents of 7.2, 8.5, and 8.8, respectively.

Fig. 2 illustrates the voltage and current unbalanced factors VUF and CUF, respectively. For low levels of voltage unbalance, the current unbalance levels are small for all the IMs. However a small change in the voltage unbalance is associated with a large change in current unbalance. Comparing the IMs, the negative sequence current in the IE4 IM grow faster than the negative sequence current in the IE3 IM and IE1 IM.
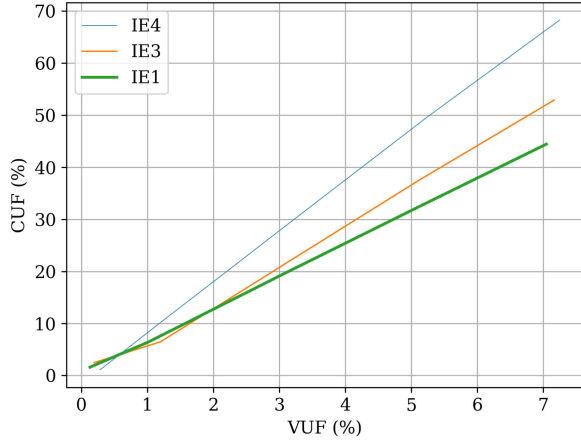
Fig. 2.   Current unbalance due to voltage unbalance in a standard efficiency class IM (IE1), a premium efficiency class IM (IE3), and a super-premium efficiency class IM (IE4).
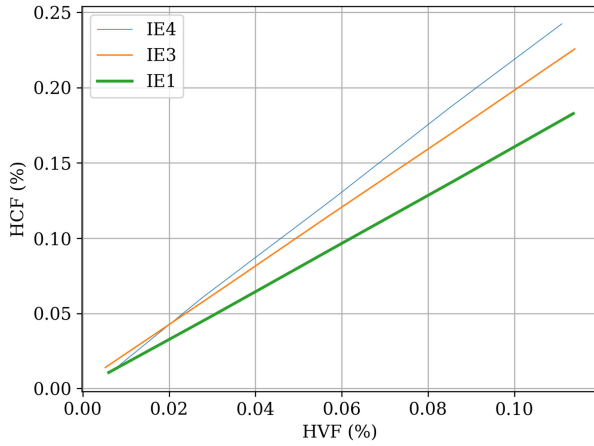

Fig. 3.   Harmonic current due to harmonic voltage in a standard efficiency class IM (IE1), a premium efficiency class IM (IE3), and a super-premium efficiency class IM (IE4).

Higher starting currents (in p.u.) are also correlated with lower impedances to harmonic components.

Fig. 3 shows the relation between the harmonic current factor and the HVF for the IMs under test. For low levels of harmonic voltage distortion, the current distortion levels are small for all the IMs. The figure shows that the harmonic currents grow faster than the percentage of harmonic voltages. Again, comparing the IMs, we see that the magnitude of the harmonic currents is higher in the IE4 IM than the IE3 and IE1 IM, which implies that the impedances to harmonic voltages are lower in the IE4 class IM than in the IE3 and IE1 IMs.

III. IM MODEL AND PARAMETERS FOR VOLTAGE UNBALANCE AND HARMONIC DISTORTION

A. IM Model for Voltage Unbalance and Harmonic Distortion

The steady state model of an IM may be used to evaluate the IM's behavior under voltage unbalance and harmonic distortion conditions [24]. The model consists of single-phase equivalent
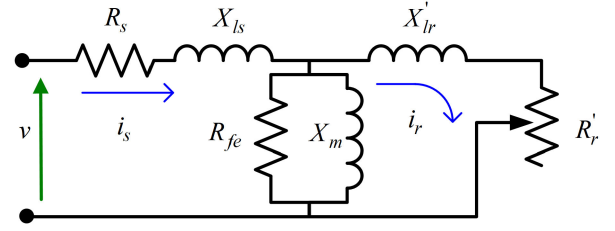

Fig. 4.   IM model equivalent single-phase circuit.

TABLE II
POSITIVE- AND NEGATIVE-SEQUENCE PARAMETER FOR THE
FUNDAMENTAL FREQUENCY

Parameter	*Fundamental frequency*	
	Positive sequence	Negative sequence
R_s	r_s	r_s
X_{ls}	x_s	x_s
R_r'	$\dfrac{r_r}{s}$	$\dfrac{r_{r1n}}{2-s}$
X_{lr}'	x_r	x_{r1n}
X_m	x_m	x_m
R_{fe}	r_{fe}	r_{fe}

TABLE III
POSITIVE- AND NEGATIVE- SEQUENCE PARAMETER FOR
HARMONIC FREQUENCIES

Parameter	*Harmonic*	
	Positive sequence	Negative sequence
R_s	r_{shp}	r_{shn}
X_{ls}	$h_p \cdot x_s$	$h_n \cdot x_{shn}$
R_r'	$\dfrac{h_p}{(h_p-1)+s}r_{rhp}$	$\dfrac{h_n}{(h_n+1)-s}r_{rhn}$
X_{lr}'	$((h_p-1)+s)\cdot x_{rhp}$	$((h_p+1)-s)\cdot x_{rhn}$
X_m	$h_p \cdot x_m$	$h_n \cdot x_m$
R_{fe}	r_{fe}	r_{fe}

circuits for the positive- and negative-sequence components of the fundamental frequency and single-phase equivalent circuits for the positive- and negative-sequence components for each harmonic frequency [24], [27], [28].

Fig. 4 shows the single-phase circuit used in the model. While the circuit topology remains the same, parameter values are different for each sequence and frequency component, as shown in Tables II and III.

Subscripts *p* and *n* indicate that the parameter corresponds to the positive or negative sequence, respectively. Similarly, *h* represents the harmonic index, e.g., $h = 5, 7$.

To compute the output power of the IM, we sum the positive sequence power and the negative sequence power for the fundamental frequency and its harmonics as follows:

$$P_{\text{output}} = P_{1p} + P_{1n} + P_{hp} + P_{hn} \tag{3}$$

where

$$P_{1p} = 3(I_{r1p})^2 \left(\frac{1-s}{s}\right) r_r \tag{4}$$

$$P_{1n} = 3(I_{r1n})^2 \frac{(s-1)}{(2-s)} r_{r1n} \tag{5}$$

$$P_{hp} = \sum_{h=6k+1}^{\infty} 3(I_{rhp})^2 \frac{h_p}{(h_p-1)+s} r_{rhp} \quad \forall k \in N \tag{6}$$

$$P_{hn} = \sum_{h=6k-1}^{\infty} 3(I_{rhn})^2 \frac{h_n}{(h_n+1)-s} r_{rhn} \quad \forall k \in N. \tag{7}$$

The losses of an IM include the stator loss, rotor loss, core loss, friction and windage loss, and stray-load loss [29]

$$p_{\text{losses}} = p_{cus} + p_{cur} + p_{fe} + p_{f+w} + p_{ll} \tag{8}$$

where

$$p_{cus} = 3(I_{s1p})^2 r_s + 3(I_{s1n})^2 r_s + \sum_{h=6k+1}^{\infty} 3(I_{shp})^2 r_{shp}$$

$$+ \sum_{h=6k-1}^{\infty} 3(I_{shn})^2 r_{shn} \tag{9}$$

$$p_{cur} = 3(I_{r1p})^2 r_r + 3(I_{r1n})^2 r_{r1n} + \sum_{h=6k+1}^{\infty} 3(I_{rhp})^2 r_{rhp}$$

$$+ \sum_{h=6k-1}^{\infty} 3(I_{rhn})^2 r_{rhn} \tag{10}$$

$$p_{fe} = 3(I_{fe1p})^2 r_{fe} + 3(I_{fe1n})^2 r_{fe}$$

$$+ \sum_{h=6k+1}^{\infty} 3(I_{fehp})^2 r_{fe} + \sum_{h=6k-1}^{\infty} 3(I_{fehn})^2 r_{fe} \tag{11}$$

$$p_{f+w} + p_{ll} = \text{constant}. \tag{12}$$

The friction, windage, and stray load losses are assumed constant because their variations are small as shown in the validation (see Section IV) [30].

B. Parameters of the IMs Under Test

We tested three 5.5 kW 50 Hz IMs, a standard efficiency class (IE1), a premium efficiency class (IE3), and a super-premium efficiency class (IE4). Table I summarizes nameplate data of each IM. Comparing starting currents of the IMs, we predict that the super-premium-efficiency IM will be more affected by voltage disturbances than the premium-efficiency IM. Finally, standard-efficiency IM will be the least affected IM by voltage disturbances.

Table IV summarizes the nominal frequency parameters of the IMs we tested in this article. To obtain these parameters, we followed the procedure described in IEEE 112-2004 standard [29].

This table shows that stator resistance r_s and rotor resistance r_r of the super-premium-efficiency IM (IE4) are lower than

TABLE IV
IM PARAMETERS FOR NOMINAL FREQUENCY

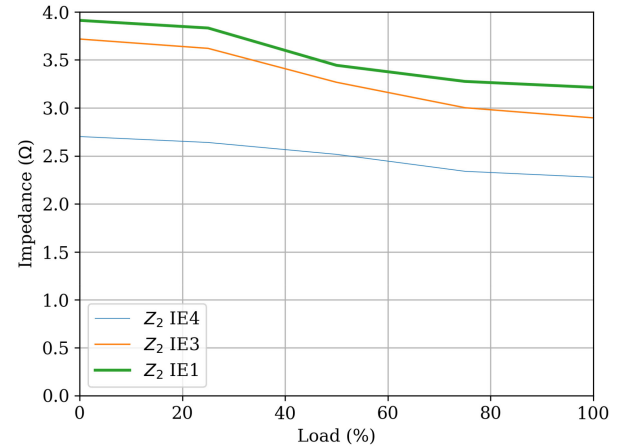| IM / Parameter (Ω)	IE1	IE3	IE4
r_s	0.896	0.633	0.594
r_r	0.331	0.247	0.229
x_s	1.683	1.462	1.207
x_r	1.683	1.462	1.207
x_m	40.73	44.76	37.01
r_{fe}	175.9	210.3	288.3

Fig. 5. Negative-sequence impedance magnitude computed from voltage and current measurements under 5% VUF.

the respective values of the premium-efficiency IM (IE3) and the standard-efficiency IM (IE1). Similarly, the stator and rotor leakage reactances of the IE4 IM are lower than those of the IE3 and IE1 IMs. On the other hand, the resistance of the magnetizing branch of the super-premium-efficiency IM (IE4) is larger than those in premium-efficiency IM (IE3) and standard-efficiency IM (IE1). The reactance of the magnetizing branch is similar in all cases.

To obtain the negative-sequence parameters, r_{r1n} and x_{r1n}, we first apply unbalanced voltages (VUF $\approx$ 5%), measure the current on the IMs, and computed the negative-sequence impedances at different loading conditions. Fig. 5 shows the impedance values we obtained. The results shown in the figure are consistent with Arkan findings in [31].

The negative sequence resistances for the IE1, IE3, and IE4 IMs were: 2.1 Ω, 1.73 Ω, 1.26 Ω, respectively, and did not change with the loading conditions. With these values, we compute the IM's model parameters as described in [28].

IV. VALIDATION OF THE MODEL AND PARAMETERS UNDER UNBALANCED VOLTAGE CONDITIONS

To validate the model and its parameters, we compared the stator current measured on a test bench with the currents obtained with the model under the same voltage and loading conditions.
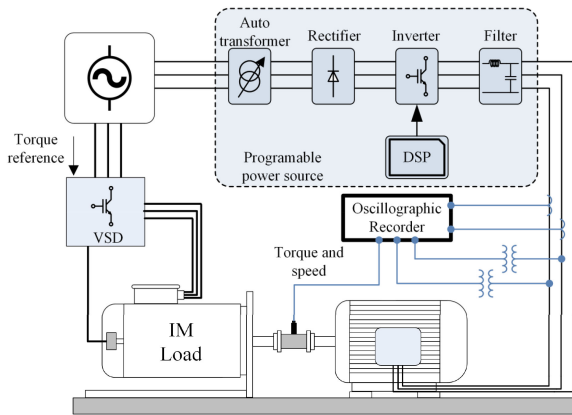
Fig. 6. Test bench used to test the IMs.

Fig. 7. IE1 IM: Measured and estimated fundamental positive-sequence current and the corresponding error, full load case.

A. Test Bench

The test bench (see Fig. 6) consists of a three-phase programmable source to create different supply voltage conditions including voltage unbalance and harmonic distortion.

Fig. 6 shows the IM under test mechanically coupled to a second IM working as a load. The IM used as load is fed by a commercial variable-speed drive, so that the load condition of the IM under test can be adjusted as required. A 0–100 N·m transducer is used to measure torque and speed. The test bench records two line voltages and two phase currents using a four channel oscillographic recorder (3.2 s, 40 kS). The remaining voltage and current are obtained from the measured values.

During the tests, we keep the positive sequence of fundamental voltage at its nominal value. Voltage unbalance is generated by incrementing the negative-sequence component of the fundamental voltage. To generate voltage distortion, we introduced 5th and 7th harmonics while maintaining the magnitude of the 7th harmonic at 0.7 times the amplitude of the 5th harmonic. Even voltage harmonics are seldom present in power systems voltages and are not included here. The third harmonic and its multiples are not included because they are zero sequence harmonics, which cannot flow into IMs due to them being either delta connected or in ungrounded wye connection.

B. Validation of the Model and Parameters Under Unbalanced Voltage Conditions

To validate the model, we measured the currents through the IMs under different conditions of voltage unbalance and load. Then, we compared these measurements with the currents predicted by the model for all the combinations of {0, 1, 3, 5, 7} percent of voltage unbalance (VUF) and {0, 25, 50, 75, 100} percent of rated load.

Using the bench described in the previous section, we measured the currents through the IMs under different conditions of voltage unbalance and load. Then, we compared these measurements with the currents predicted by the model for each voltage and load conditions.

Fig. 7 shows the measured and estimated fundamental positive-sequence currents for the IE1 IM operating at full load.
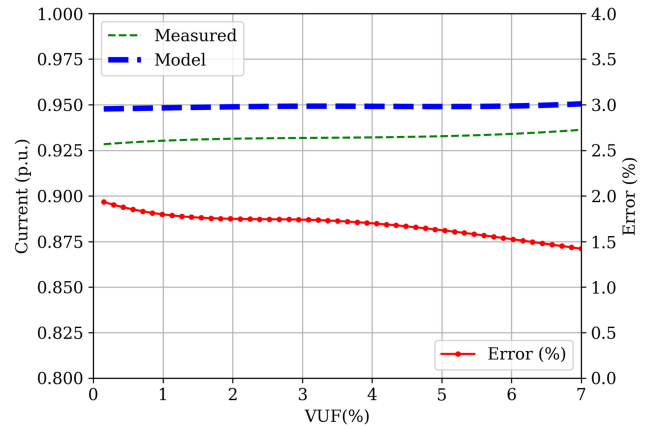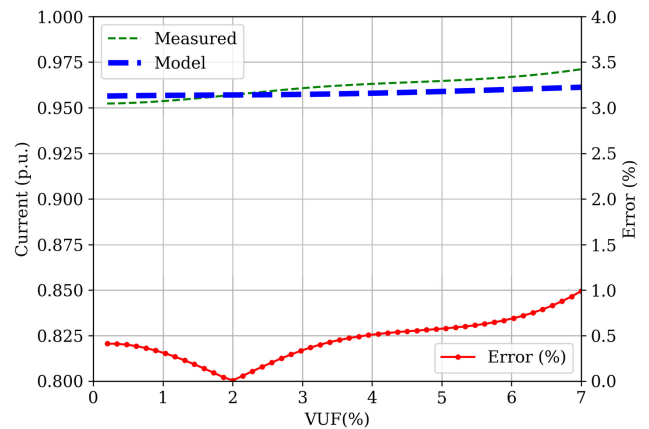

Fig. 8. IE3 IM: Measured and estimated fundamental positive-sequence current, and the corresponding error, full load case.
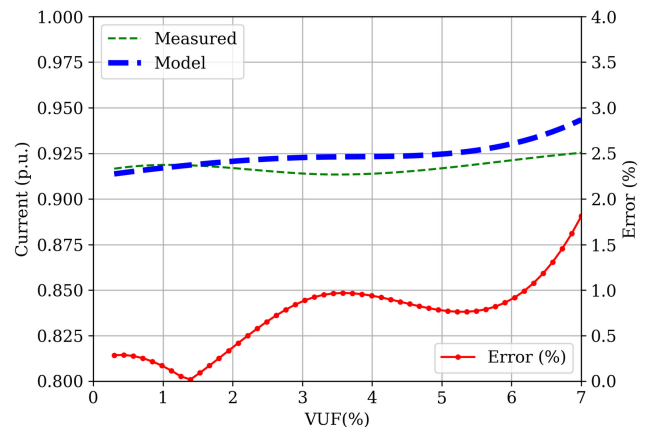

Fig. 9. IE4 IM: Measured and estimated fundamental positive-sequence current, and the corresponding error, full load case.

Figs. 8 and 9 present the same data for the IE3 IM and IE4 IM, respectively. These figures show that the differences between the measured and modeled values are less than 2%.

Fig. 10 shows the calculated and measured negative-sequence current for the IE1 MI at full load and for different levels of voltage unbalance. Figs. 11 and 12 present the same data for the IE3
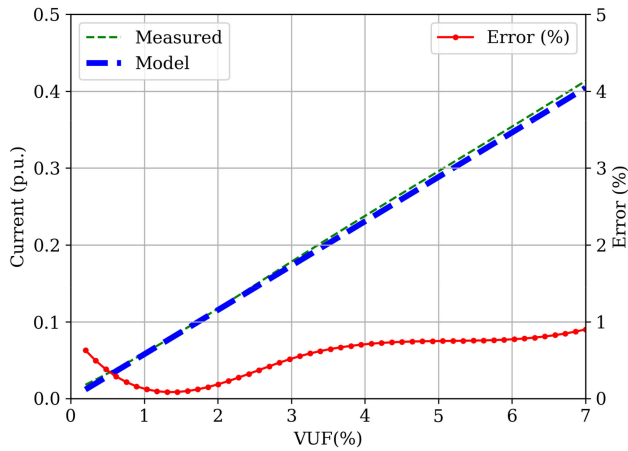
Fig. 10.   IE1 IM: Measured and computed negative-sequence fundamental current and the corresponding error, full load case.
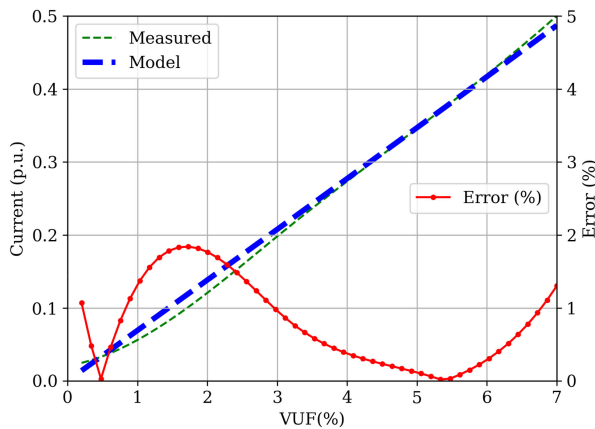

Fig. 12.   IE4 IM: Measured and computed negative-sequence fundamental current and the corresponding error, full load case.

Fig. 11.   IE3 IM: Measured and computed negative-sequence fundamental current and the corresponding error, full load case.

Fig. 13.   IE1 IM: Measured and computed negative-sequence fundamental current and the corresponding error, no load case.

IM and IE4, respectively. These figures show a proper agreement between the current obtained using the models and the measured currents. Note that the difference between the currents is below 2% of the nominal current. These figures also show that the negative-sequence currents grow linearly with the voltage unbalance level, and that a 7% of voltage unbalance leads to negative-sequence currents close to 40% of the nominal current of the standard-efficiency IM. For the premium-efficiency IM, 7% of voltage unbalance causes negative-sequence currents that reach 50% of the nominal current. In the super-premium-efficiency IM, 7% of voltage unbalance causes negative-sequence currents that reach 64% of the nominal current. This result is consistent with the analysis we presented in Section II.

The negative-sequence impedance of IMs changes with the loading level, it is then important to validate the IM model and parameters for different loading levels.

Fig. 13 shows the calculated and measured negative-sequence current for the IE1 IM at no-load condition for different levels of voltage unbalance. Figs. 14 and 15 present the same data for the IE3 IM and IE4 IM, respectively.
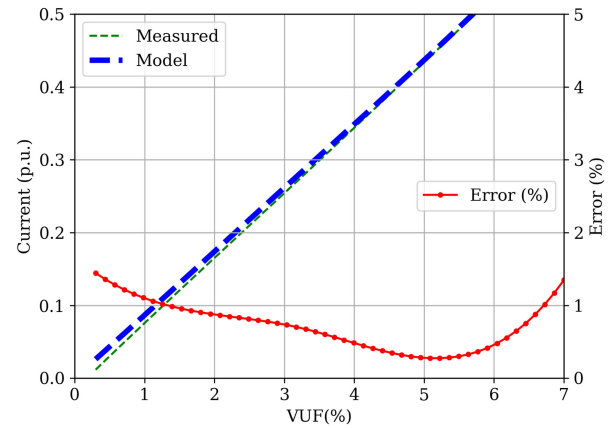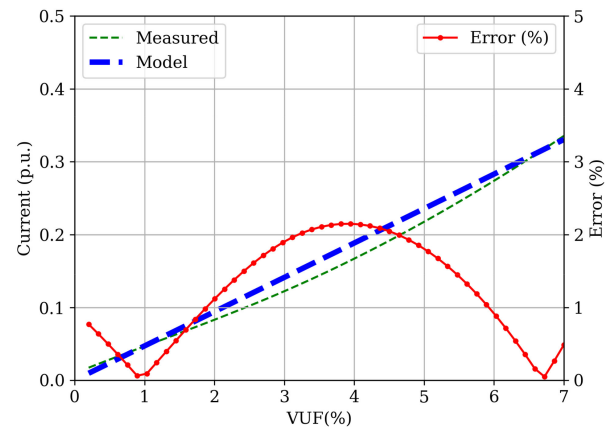
Reviewing Figs. 6–14, we see a maximum estimation error of 4.8%. These differences may be attributed to the variations in the stray losses, which we contemplate as constant in this article [30].We validated the model for loading conditions between full and no load, and we found that the model presents the same or better accuracy than in the cases shown earlier.

V. COMPARISON OF DERATING FACTORS

In this section, we used the model we validated in Section IV to obtain derating factors for the three IMs. The derating factors are calculated for different voltage unbalance and harmonic voltage conditions as described further.

A. Derating Factors for Unbalanced Voltage Conditions

According to the NEMA and IEC standards, IMs are designed to operate continually at full load with a 1% of voltage unbalance [15], [16]. We compute the total baseline losses in the IM for those conditions. Then, we increase the voltage unbalance in 0.5% steps. At each step and as a consequence of the increase in voltage unbalance, the losses in the IM increase. So, at each step we scale down the load until the losses in the IM fall back to
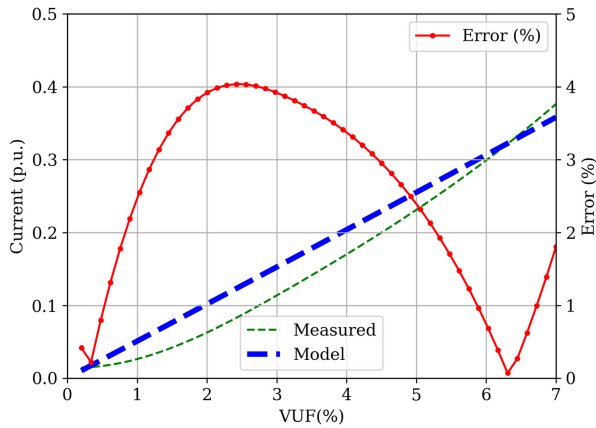
Fig. 14.   IE3 IM: Measured and computed negative-sequence fundamental current and the corresponding error, no load case.
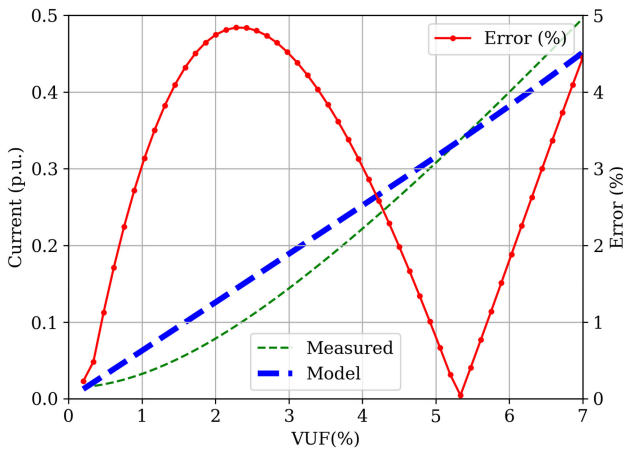

Fig. 15.   IM: Measured and computed negative-sequence fundamental current and the corresponding error, no load case.
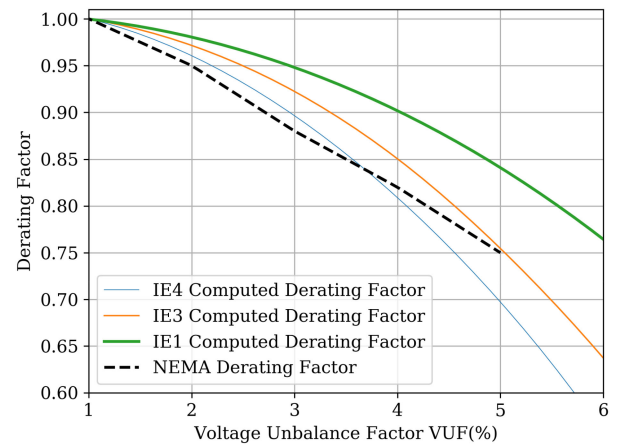

Fig. 16.   NEMA derating factors maintain IM losses below design values, but margins are smaller for the higher efficiency class IM as predicted by the lower negatives sequence impedance.
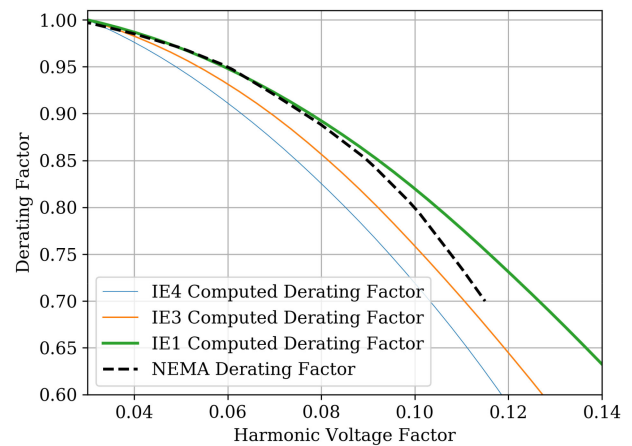

Fig. 17.   NEMA derating factors are not sufficient to maintain IM losses below design values in the IE3 and the IE4 IMs

the baseline value. These scale-down factors are the computed derating factors corresponding to the different voltage unbalance levels.

Fig. 16 compares the derating factors we computed for the IE1, IE3, and IE4 IMs with the derating factors suggested by the NEMA standard [15]. Note that while the derating factors suggested by the standard adequately protect IE1 and IE3 IMs, the margins for the IE3 IM are smaller than those for the IE1 IM as inferred from the lower negative sequence resistance on the IE3 IM. In the IE4 IM, the standard protects adequately for VUF<3.5%. For VUF>3.5%, the derating factors proposed in the standard are not enough to protect the IE4 IM.

B. Derating Factors for Harmonic Distortion Conditions

In this section, we assume that IMs can operate indefinitely at full load with a 0.03 HVF harmonic distortion condition. With this level of harmonic distortion, the IM losses are like those with the IM operating with 1% VUF. Then, we compute derating factors for HVF values between 0.03 and 0.14 HVF. We introduce 5th and 7th harmonic voltages while we maintain

the 7th harmonic at 70% the magnitude of the 5th harmonic. Fig. 17 compares the derating factors defined in NEMA standard with the derating factors we computed for the IE1, IE3, and IE4 IMs. Note that the derating factors computed for the IE1 IM are close and somewhat above the values suggested by the NEMA standard. However, the derating factors computed for the IE3 and IE4 IMs are below NEMA's values, indicating that losses in these IMs are higher than the losses for which the IMs are designed.

VI. CONCLUSION

In this article, we study the effect of voltage unbalance and harmonic distortion on the losses of IMs in different efficiency classes.

We first studied the nameplate data of 548 IMs to show that higher efficiency class IMs are correlated to higher starting currents in p.u. Then, we drew attention to the work presented in [24], where higher starting current are associated with lower

negative-sequence impedances and to higher losses for unbalanced and distorted voltage conditions.

In a second approach, we compared the behavior of three IMs (an IE1, an IE3, and an IE4 efficiency class) under harmonic and unbalanced voltage conditions. We found that, for the same levels of voltage unbalance and harmonic distortion, losses were greater in the IE4 class IM than in the IE3 class IM and IE1 class IM. For these IMs, we computed derating factors to maintain losses at the design values. The derating factors corresponding to the IE1 IM were above that suggested by the standards. However, the derating factors computed for the IE3 IM and IE4 IM are in some cases below NEMA's values, indicating that losses in the IMs are higher than the losses for which the IMs is designed.

This article suggests that 1) IM losses due to voltage unbalance and harmonic distortion are greater in higher efficiency class IMs, and 2) that derating factors defined in standards are not enough to avoid overload on higher efficiency class IMs.

REFERENCES

[1] F. J. T. E. Ferreira and A. T. d. Almeida, "Overview on energy saving opportunities in electric motor driven systems - Part 1: System efficiency improvement," in *Proc. IEEE/IAS 52nd Ind. Commercial Power Syst. Tech. Conf.*, 2016, pp. 1–8.

[2] F. J. T. E. Ferreira and A. T. de Almeida, "Overview on energy saving opportunities in electric motor driven systems - Part 2: Regeneration and output power reduction," in *Proc. IEEE/IAS 52nd Ind. Commercial Power Syst. Tech. Conf.*, 2016, pp. 1–8.

[3] V. Dmitrievskii, V. Prakht, and V. Kazakbaev, "IE5 energy-efficiency class synchronous reluctance motor with fractional slot winding," *IEEE Trans. Ind. Appl.*, vol. 55, no. 5, pp. 4676–4684, Sep./Oct. 2019.

[4] A. T. de Almeida, F. J. T. E. Ferreira, and G. Baoming, "Beyond induction motors-technology trends to move up efficiency," *IEEE Trans. Ind. Appl.*, vol. 50, no. 3, pp. 2103–2114, May/Jun. 2014.

[5] R. Sperberg, R. Kniss, and T. Ruegg, "Energy efficiency in california cement plants: Energy savings potential realized by accessing utility energy-efficiency program resources," *IEEE Ind. Appl. Mag.*, vol. 24, no. 4, pp. 12–16, Jul./Aug. 2018.

[6] F. J. T. E. Ferreira, G. Baoming, and A. T. de Almeida, "Reliability and operation of high-efficiency induction motors," *IEEE Trans. Ind. Appl.*, vol. 52, no. 6, 4628–4637, Nov./Dec. 2016.

[7] P. Gnaciński, M. Pepliński, D. Hallmann, and P. Jankowski, "Induction cage machine thermal transients under lowered voltage quality," *IET Electric Power Appl.*, vol. 13, pp. 479–486, 2019.

[8] D. Zhang, R. An, and T. Wu, "Effect of voltage unbalance and distortion on the loss characteristics of three-phase cage induction motor," *IET Electric Power Appl.*, vol. 12, pp. 264–270, 2018.

[9] E. B. Agamloh, A. Cavagnino, and S. Vaschetto, "Standard efficiency determination of induction motors with a PWM inverter source," *IEEE Trans. Ind. Appl.*, vol. 55, no. 1, pp. 398–406, Jan./Feb. 2019.

[10] A. L. Van Wyk, M. A. Khan, and P. Barendse, "Impact of over/under and voltage unbalanced supplies on energy-efficient motors," in *Proc. IEEE Int. Electric Machines Drives Conf.*, 2011, pp. 1380–1385.

[11] M. D. de Castro e Silva, A. L. Ferreira Filho, A. B. F. Neves, and M. V. B. Mendonça, "Effects of sequence voltage components on torque and efficiency of a three-phase induction motor," *Electric Power Syst. Res.*, vol. 140, pp. 942–949, May 2016.

[12] P. Donolo, G. Bossio, C. De Angelo, G. García, and M. Donolo, "Voltage unbalance and harmonic distortion effects on induction motor power, torque and vibrations," *Electric Power Syst. Res.*, vol. 140, pp. 866–873, 2016.

[13] E. El-Kharashi, M. El-Dessouki, J. G. Massoud, A. W. Farid, and M. A. Al-Ahmar, "The use of the current complex factor to determine the precise output energy of the induction motor," *Electric Power Syst. Res.*, vol. 154, pp. 23–36, 2018.

[14] *IEEE Recommended Practice for Electric Power Distribution for Industrial Plants*, IEEE 141-1993, 1993.

[15] *NEMA Standards Publication ANSI/NEMA MG 1-2003, Revision 1-2004: Motors and Generators*, NEMA National Electrical Manufacturers Association, 2003.

[16] *Rotating Electrical Machines - Part 26: Effects of Unbalanced Voltages on the Performance of Three-Phase Cage Induction Motors Standard*, IEC 60034-26, International Electrotechnical Commission, Geneva, Switzerland, 2006.

[17] J. P. G. de Abreu and A. E. Emanuel, "Induction motors loss of life due to voltage imbalance and harmonics: A preliminary study," in *Proc. Harmonics Qual. Power, Proc. 9th Int. Conf.* , 2000, vol. 1, pp. 75–80.

[18] C. A. Reineri, J. C. Gomez, E. B. Belenguer, and M. Felici, "Revision of concepts and approaches for unbalance problems in distribution," in *Proc. Transmiss. Distrib. Conf. Expo. : Latin America, TDC '06. IEEE/PES*, 2006, pp. 1–6.

[19] P. Gnacinski and T. Tarasiuk, "Energy-efficient operation of induction motors and power quality standards," *Electric Power Syst. Res.*, vol. 135, pp. 10–17, 2016.

[20] P. Donolo, M. Pezzani, G. Bossio, E. C. Quispe, D. Valencia, and V. Sousa, "Impact of voltage waveform on the losses and performance of energy efficiency induction motors," in *Proc. IEEE ANDESCON*, 2018, pp. 1–4.

[21] R. Kanchan, R. Chitroju, and F. Gyllensten, "Evaluation of efficiency measurement methods for sinusoidal and converter fed induction motors," in *Proc. 8th Int. Conf. Energy Efficiency Motor Driven Syst.*, 2013, pp. 1–8.

[22] *IEEE Recommended Practice for Motor Protection in Industrial and Commercial Power Systems*, IEEE 3004.8-2016, May 2017.

[23] P. Donolo, C. Pezzani, G. Bossio, C. de Angelo, and M. Donolo, "Derating of induction motors due to power quality issues considering the motor efficiency class," *IEEE Industry Applications Society Annual Meeting*, Baltimore, MD, USA, 2019, pp. 1–6, doi: 10.1109/IAS.2019.8912435.

[24] R. C. Dugan, M. F. McGranaghan, S. Santoso, and H. W. Beaty, *Electrical Power Systems Quality*, 3rd ed. New York, NY, USA: McGraw-Hill, 2012.

[25] F. J. T. E. Ferreira, B. Leprettre, and A. T. de Almeida, "Comparison of protection requirements in IE2-, IE3-, and IE4-class motors," *IEEE Trans. Ind. Appl.*, vol. 52, no. 4, pp. 3603–3610, Jul./Aug. 2016.

[26] "Electric motors for general purpose W22," 2019. [Online]. Available: http://ecatalog.weg.net/tec_cat/tech_motor_sel_web.asp

[27] V. S. Santos, P. R. V. Felipe, J. R. G. Sarduy, N. A. Lemozy, A. Jurado, and E. C. Quispe, "Procedure for determining induction motor efficiency working under distorted Grid voltages," *IEEE Trans. Energy Convers.*, vol. 30, no. 1, pp. 331–339, Mar. 2015.

[28] P. Donolo, G. Bossio, and C. De Angelo, "Analysis of voltage unbalance effects on induction motors with open and closed slots," *Energy Convers. Manage.*, vol. 52, pp. 2024–2030, 2011.

[29] *IEEE Standard Test Procedure for Polyphase Induction Motors and Generators*, IEEE Std 112-2004 (Revision IEEE Std 112-1996), 2004.

[30] M. Dems, K. Komeza, and J-Ph Lecointe. "Variation of additional losses at no-load and full-load for a wide range of rated power induction motors," *Electric Power Syst.Res.*, vol. 143, pp. 692–702, 2017.

[31] M. Arkan, D. Kostic-Perovic, and P. Unsworth, "Closed rotor slot effect on negative sequence impedance [in induction motors]," in *Proc. Conf. Record Ind. Appl. Conf.*, 2001, pp. 751–753.

Pablo D. Donolo (Member, IEEE) received the graduate degree in electrical engineering, in 2006, the M.S. degree in engineering sciences, in 2013, and the doctorate degree in engineering sciences, in 2014, from the Universidad Nacional de Río Cuarto, Río Cuarto, Argentina.

In 2005, he joined the Grupo de Electrónica Aplicada, Universidad Nacional de Río Cuarto. He is currently an Assistant Professor with the Universidad Nacional de Río Cuarto and an Assistant Researcher with the Consejo Nacional de Investigaciones Científicas y Técnicas, Buenos Aires, Argentina. His research interests include energy efficiency, power quality, and fault diagnosis on electric machines.

Carlos M. Pezzani (Member, IEEE) received the degree in electrical engineering, in 2007, and the doctorate degree in engineering sciences, in 2013, from the Universidad Nacional de Río Cuarto, Río Cuarto, Argentina.

In 2007, he joined the Grupo de Electrónica Aplicada, Universidad Nacional de Río Cuarto. He is currently an Assistant Professor with the Universidad Nacional de Río Cuarto and an Assistant Researcher with the Consejo Nacional de Investigaciones Científicas y Técnicas, Buenos Aires, Argentina. His research interests include fault diagnosis on electric machines and energy efficiency.

Cristian H. De Angelo (Senior Member, IEEE) received the degree in electrical engineering from the Universidad Nacional de Río Cuarto, Río Cuarto, Argentina, in 1999, and the doctorate degree in engineering services from the Universidad Nacional de La Plata, Argentina, in 2004.

In 1994, he joined the Grupo de Electrónica Aplicada, Universidad Nacional de Río Cuarto. He is currently an Associate Professor with the Universidad Nacional de Río Cuarto and the Principal Researcher with the Consejo Nacional de Investigaciones Científicas y Técnicas, Buenos Aires, Argentina. His research interests include electric and hybrid vehicles, fault diagnosis on electric machines, electric motors control, and renewable-energy generation.

Guillermo R. Bossio (Senior Member, IEEE) received the degree in electrical engineering from the Universidad Nacional de Río Cuarto, Río Cuarto, Argentina, in 1999, and the doctorate degree in engineering sciences from the Universidad Nacional de La Plata, Buenos Aires, Argentina, in 2004.

Since 1994, he has been with the Grupo de Electrónica Aplicada, Facultad de Ingeniería, Universidad Nacional de Río Cuarto. He is currently an Associate Professor with the Universidad Nacional de Río Cuarto and an Independent Researcher with the Consejo Nacional de Investigaciones Científicas y Técnicas, Buenos Aires, Argentina. His research interests include fault diagnosis of electric machines, ac motor drives, electric vehicles, and renewable energy generation.

Marcos A. Donolo (Senior Member, IEEE) received the B.S.E.E. degree from the Universidad Nacional de Río Cuarto, Río Cuarto, Argentina, in 2000, the M.S. degree in electrical engineering and mathematics, and the Ph.D. degree in electrical engineering from Virginia Polytechnic Institute and State University, in 2002, 2005, and 2006, respectively.

Since 2006, he has been with Schweitzer Engineering Laboratories, Inc., Pullman, WA, USA, where he is currently a Principal Engineer. He holds several patents and has authored numerous papers related to power system protection.